Ring electrode for radiofrequency heating of the cornea: modelling and *in vitro* experiments

Enrique J. Berjano[1], Javier Saiz[1], Jorge L. Alió[2], José M. Ferrero[1]

[1] Electronic Engineering Department, Valencia Polytechnic University, Valencia, Spain.

[2] Surgery Department, Miguel Hernández University School of Medicine, Alicante, Spain

Correspondence should be addressed to:

Prof. Enrique J. Berjano

Departamento de Ingeniería Electrónica. Universidad Politécnica de Valencia

Camino de Vera s/n, 46022 Valencia, SPAIN

Phone. 3496-3877607 Fax: 3496-3877609

E-mail: eberjano@eln.upv.es

Abstract – Radiofrequency thermokeratoplasty (RF-TKP) is a technique used to reshape the cornea curvature by means of thermal lesions using radiofrequency currents. This curvature change allows to correct refractive disorders such as hyperopia. We propose a new electrode with ring geometry for RF-TKP. It was designed to create a single thermal lesion with full circle shape. We developed finite element models and analysed the temperature distributions in the cornea for different ring electrode characteristics. The computer results indicated that the maximal temperature in the cornea located in the vicinity of the ring electrode outer perimeter, and that the lesions had a semi-torus shape. The results also indicated that the electrode thickness, electrode radius, and electrode thermal conductivity have a significant influence on the temperature distributions. In addition, we performed *in vitro* experiments on rabbit eyes. At a 5 W power, the lesions were fully circular. Some lesions showed non uniform characteristics along their circular path. Lesion depth depended on heating duration (60% of corneal thickness for 20 s, and 30% for 10 s). The results suggest that the critical shrinkage temperature (55-63ºC) was reached at the central stroma and along the entire circular path in all the cases.

Keywords – Computer model, cornea, hyperopia, finite element method, numerical model, radiofrequency, ring electrode, theoretical model, thermokeratoplasty.

1 Introduction

Radiofrequency thermokeratoplasty (RF-TKP) is a technique used to reshape the cornea curvature by means of thermal lesions using radiofrequency currents. In RF-TKP, temperature of the stromal layer of the cornea is elevated to its shrinkage temperature of 55-63ºC (STRINGER and PARR, 1964) by absorption of energy. When the lesion pattern is suitable, the shrinkage of collagen in the stromal layer can change the surface curvature of the cornea in a controlled way (TREMBLY *et al.*, 2001). Several groups have proposed the use of radiofrequency (RF) currents for creating heating in TKP (DOSS AND ALBILLAR, 1980; MÉNDEZ-G and MÉNDEZ-NOBLE, 1997; ASBELL *et al.*, 2001). In 1980, DOSS and ALBILLAR (1980) proposed a TKP technique with RF currents (RF-TKP) using a large diameter electrode combined with surface cooling in order to correct the keratoconus. The clinical results using this technique showed unpredictability and regression of the shrinkage effect (ROWSEY, 1987). Recently, MENDEZ-G and MENDEZ-NOBLE (1997) have proposed a RF-TKP technique for the correction of hyperopia using a smaller diameter electrode (single probe) without surface cooling. This new technique is called conductive keratoplasty (CK), and is based on creating a circle of lesion spots on the cornea surface. The first clinical results achieved that hyperopia correction was stable and had little regression through time (ASBELL *et al.*, 2001; MCDONALD *et al.*, 2002).

In early work (BERJANO *et al.*, 2002), we presented a theoretical model based on finite element method for the study of RF-TKP using a single probe. In that work, we studied the effect of the tissue characteristics (such as anisotropy of the cornea thermal conductivity, or presence of a tear film on the cornea) and electrode characteristics (insertion depth of the active electrode in the cornea). The computer results suggested that these effects had a significant influence on the temperature distributions and thereby on the lesion dimensions. We also carried out *in vitro* experiments on rabbit eyes and we observed a tendency towards the agreement between experimental and theoretical results, although the theoretical model overestimated the lesion dimension.

Up to now, clinical studies (ASBELL *et al.*, 2001; MCDONALD *et al.*, 2002) have demonstrated that CK procedure allows to correct low to moderate hyperopia (from +0.75 to +3.00 diopters). However, an experimental study showed that the application of heated brass rings (6-7 mm diameter) on enucleated bovine eyes provoked predictable increases of corneal refracting power of 4 to 14 diopters (MILLER and MANNING, 1978). Later, another experimental study in living rabbits used equally brass rings heated (98 – 110ºC, 5 s) and a significant increase of corneal curvature of up to 10.5 diopters was induced (GRUENBERG *et al.*, 1981). Although this change tended to be transient, DOSS and ALBILLAR (1980) demonstrated that the use of heated probes (90ºC) does not allow to reach the critical shrinkage temperature (55-63ºC) at central stroma. Since that it is known that a little deep corneal lesion can produce regression in some cases (MÉNDEZ-G and MÉNDEZ-NOBLE, 1997), this limitation in the penetration of the lesion could be the cause of the transient results obtained by GRUENBERG *et al.* (1981).

There is no past research supporting some advantage of a RF ring electrode as contrasted with a single RF probe. Nevertheless, previous work on heated brass rings suggests that the creation of a fully circular lesion and with sufficient depth along the entire circular path, would present some advantages for hyperopia correction. To our knowledge, there is only one technical document proposing a ring electrode for RF heating of the cornea (SILVESTRINI, 1998), but it is not for surface application, and there are no associated theoretical, experimental or clinical results.

In this paper, we present a theoretical model for the simulation of corneal temperature distribution during RF-TKP using a ring electrode of surface application. The first objective of our work has been to use the theoretical model in order to study the effect of different electrode characteristics on the temperature profile and thereby on the lesion. The second objective has been to investigate the geometry and characteristics of the lesions by means of computer simulations and *in vitro* experiments on isolated rabbit eyes; in this way, it has been possible to assess the capabilities of the ring electrode for creating a lesion of fully circular shape and sufficiently deep.

This investigation is a step forward in the development of a new electrode for RF heating of the cornea. However, it is necessary to point out that it is a preliminary stage, and therefore, subsequent experimental and clinical studies should be performed to assess the practicality (stable and reproducible refractive changes) and safety of the proposed device.

2 Materials and methods

2.1 *Description of the theoretical model*

In RF-TKP, electrical currents (500 kHz to 1 MHz) flow between an active electrode placed on the cornea surface and a dispersive electrode of large dimensions placed on the back of the patient’s head. We constructed an active electrode with ring geometry made of stainless steel and with a 7 mm inner diameter. Since the ring electrode is located in the centre of the cornea, the theoretical model presents axisymmetric characteristics, and a two-dimensional approach is possible. Fig. 2 shows the theoretical model proposed. It represents a fragment of ring electrode, cornea and aqueous humor (fluid included in the anterior chamber). The length of the sharp-edge zone of the active electrode (H) is 5 mm, the thickness of its body (W) is 1 mm, its radius (T) is 3.5 mm, and its thickness in the point placed on the cornea (S) is 200 μm. Corneal thickness (C) was considered of 600 μm (TREMBLY and KEATES, 1991). The value of the model parameters L, R and Z were calculated by sensitivity analysis in order to avoid boundary effects, which will be presented in Section 3.

Table 1 shows the electrical and thermal characteristics of the materials used in the model (BERJANO *et al.*, 2002). The interface between the cornea and air has been referred to the epithelium, and the interface between the cornea and the aqueous humor as the endothelium. In our model, we considered a change of the electrical conductivity of the cornea and the aqueous humor with temperature of +2%·$^{\circ}C^{-1}$ (SCHWAN and FOSTER, 1980).

We used the finite element method (ANSYS University 6.0 commercial finite element package running on an IBM-PC with a 667-MHz processor) to calculate the temperature profiles for RF-TKP. The temperature distribution in the tissue was obtained by solving the equation governing electric and thermal phenomena during RF heating of biological tissues (see Appendix). The model presented is based on a time domain analysis of an electric-thermal coupled problem, and is similar to numerical models of radiofrequency heating of biological tissue used by others authors (PANESCU *et al.*, 1995; LABONTÉ, 1994). The temperature for the surfaces away from the active electrode (right and bottom limit of the model in the Fig. 2) was assumed to be 20ºC (Dirichlet boundary conditions). An initial temperature of 20ºC was used in the entire model. The effect of heat convection in the interfaces epithelium and endothelium have been taken into account using different thermal transfer coefficients (h_1=20 W·m^{-2}·$^{\circ}C^{-1}$ for the epithelium and h_2=500 W·m^{-2}·$^{\circ}C^{-1}$ for the endothelium) (BERJANO *et al.*, 2002) and the effect of heat convection at the ring electrode-air interface, using a thermal transfer coefficient of 20 W·m^{-2}·ºC^{-1}. At these three interfaces the temperature obeys

$$\nabla T \cdot \boldsymbol{dS} = \mathrm{h} \cdot k^{-1} \cdot (T_b - T) \qquad (1)$$

where T is the tissue temperature, $\boldsymbol{S}$ is the directed surface, k is the thermal conductivity of the tissue, h is the thermal transfer coefficient, and T_b is the temperature far from the interfaces (air temperature for epithelium interface, and tissue quiescent temperature for the endothelium interface). We fixed the electrical potential on the active electrode to a value equal to the total applied voltage (root-mean-square value in an experimental set-up), while the potential in the dispersive electrode was fixed to zero volts.

We used the value of the maximal temperature achieved in the tissue (T_{max}) as a control parameter in the sensitivity analysis. In order to assess the effect of different factors studied in this work, we used the same method described in BERJANO *et al*. (2002): An effect was considered significant when the inclusion of this factor induced a change of ±4ºC in T_{max}. Finally, we characterised the geometry of the temperature profiles by means of the depth and width of the 40ºC isothermal line.

2.2 *Description of the experimental model*

We developed an *in vitro* model based on an isolated rabbit eye in order to study the lesion characteristics created with the ring electrode. Fig. 3 shows the experimental arrangement of this model which is similar to that used by DOSS and ALBILLAR (1980). We used a RF generator (model 1500-T4, Irvine Biomedical Inc., CA, USA) to deliver 500 kHz RF currents to the tissue with a 5 W power. Actually, this device uses a constant voltage mode, and thus this power level corresponded to 22.4 V. The time duration was initially set to 20 s, however RF current delivery was automatically stopped by the generator when the electrical impedance increased suddenly over 250 Ω. The experiments were carried out on enucleated rabbit eyes. After heating, the cornea was excised from the eye, preserved in formalin, sliced at 4 μm thickness through the centre of the lesion, and stained with hematoxylin and eosin. We assessed the lesion geometry by mean of the coagulation contour. The depth and width of each lesion (indicated as % of corneal thickness) were measured on the histologic samples under an optical microscope (×100). More details are described in BERJANO *et al.* (2002).

3 Results and discussion

3.1 *Construction of the theoretical model*

A section of the theoretical model can be constructed since physical dimensions such as the electrode thickness (S) or its radius (T) are known. Nevertheless, the parameters R, Z and L of the model (Fig. 2) can not be inferred from the actual physical dimensions, because only a portion of the physical stage is included in the theoretical model. In order to avoid numerical artefacts in the FEM model, we tested the model by increasing the value of these parameters. We programmed a voltage of 20 V and duration of 1 s. Computer simulations were made increasing equally the value of R and Z from 1 mm to 15 mm in steps of 1 mm. When the difference between the maximal temperature achieved in the tissue (T_{max}) after 1 s, and the temperature in the previous simulation was less than ±0.5ºC, we considered the former values of R and Z to be adequate. A value of 10 mm was obtained for R and Z. We used the same method to estimate the minimum value of L. Values from 0.5 to 5 mm in steps of 0.5 mm were used, and an optimum value of 3 mm was obtained. The time step used for all the transient analysis was set to 50 ms. The difference between T_{max} obtained with this step time and one with a low step time (25 ms) was less than ±0.5ºC. We have used a Cauchy convergence test to determine whether the model mesh is of appropriate size. This method has been described by TUNGJITKUSOLMUN *et al.* (2000) in a RF cardiac ablation model. We considered the maximal temperature in all the tissue as the parameter for the convergence test. A grid size of 10 μm in the finest zone (cornea–active electrode interface) was found to be adequate. On the contrary, the spatial resolution was of 0.6 mm near the dispersive electrode. The finite element model had nearly 2300 nodes and used over 4300 triangular elements.

3.2 *Electro-thermal behaviour of the ring electrode*

We carried out computer simulations to study the electrical and thermal behaviour of the ring electrode. Output voltage was programmed to 20 V during 1 s. Fig. 4 shows the time evolution of temperature distribution in the cornea. The maximum temperature in the tissue is always located near the outer perimeter of the ring electrode, and from this point, the isothermal lines enlarge towards deeper region of the cornea when the heating duration increases.

The main conclusion of the simulations is that the geometry of the isothermal lines is non symmetric around the electrode. That it is due to the electric field (**E**) distribution in a very small region around a ring electrode (see Fig. 5). Exactly, the highest value of **E** in the cornea zone is located near the outer perimeter of the electrode, and this fact provokes that the highest current density in the cornea is also located in this zone. This tendency of the current density towards this outer zone is similar to that obtained by WILEY and WEBSTER (1982) in an analysis of the current distribution under circular electrodes. This agreement between both studies is due to the value of **E** in the inner zone of the ring electrode (see Fig. 1) being smaller than at the outer part of the ring. This phenomenon has also been observed in a recent theoretical study on the current density distribution under electrodes for external defibrillation (KRASTEVA and PAPAZOV, 2002); especially in the case of a circular electrode with aeration openings.

On the other hand, electrodes with loop or ring shape have been proposed to create thermal lesions in atrial tissue (AVITALL *et al.*, 1999; HATA *et al.*, 2001). However, to our knowledge, there are no theoretical studies on the current density with these types of electrodes. MCRURY *et al.* (1997) studied theoretically the temperature distributions during RF cardiac ablation using a long electrode with straight shape. They observed that the current density distribution in the tissue was non uniform and concentrated in the two extreme zones. This fact has been called “edge effect” (MIROTZNIK and SCHWARTZMAN, 1996; MCRURY *et al.*, 1997). If a long electrode with straight shape is curved until it forms a ring or a loop, it would be possible to suppose that the edge effect vanished. The result of our study suggests the opposite. The geometry of the proposed ring electrode is different from the long electrode with straight shape used in RF cardiac ablation; however our result suggests that when loop or ring electrodes are used, a new edge effect appears in the outer perimeter of the electrode.

In spite of this edge effect in the outer perimeter of a ring electrode, the geometry of the 40ºC isothermal line observed in the temperature distribution of Fig. 4, suggests that it would be possible to create deep thermal lesions with a semi-torus shape. This was also observed experimentally in our study (see section 3.6), and it could be due to that the inner perimeter of the ring electrode shows a sufficient value of electrical current (see Fig. 5) to increase the temperature in this zone.

3.3 *Effect of the electrode thickness*

We studied the effect of change in two parameters related to the electrode geometry: electrode thickness (S in Fig. 2), and electrode radius (T in Fig. 2, see section 3.4). We carried out three computer simulations programming a 20 V output voltage during 1 s, and increasing the electrode thickness (S) from 50 to 300 μm (with the same electrode radius T=3.5 mm). Table II shows the effect of this change on T_{max} and on the depth and width of the 40ºC isotherm line. When electrode thickness was increased, a lower value of T_{max} and smaller dimensions of the 40ºC isothermal were achieved. Furthermore, as electrode thickness was increased from 50 to 300 μm, T_{max} decreased from 71.9 to 50.4ºC, the width of the 40ºC isothermal line decreased from 1070 to 911 μm, and the depth decreased from 490 to 380 μm. In conclusion, the change in electrode thickness has a significant effect on the temperature distributions. This result suggests that when the thickness of the ring electrodes is reduced, it is possible to create bigger lesions and the maximum temperature in the cornea is increased. In our study, when electrode thickness increased from 50 to 300 μm, there was a larger contact area between tissue and electrode, and thus the total impedance value decreased from 52.6 to 41.9 Ω (in t = 0 s). Since we programmed a constant output voltage, this change in the total impedance involved an increase of the total RF current from 380 to 477 mA (t=0 s), and the maximum current density in the tissue decreased from 174 to 144 $mA{\cdot}mm^{-2}$ (t=1 s). In conclusion, our simulations showed that the effect of the maximum current density in the tissue was more important that the effect of the total RF current.

Additionally, the current density was the main cause of the change in T_{max}, and as a consequence in lesion dimension.

3.4 *Effect of the electrode radius*

In the circular lesions pattern suggested by ASBELL *et al.* (2001) to correct hyperopia using RF currents, several lesion spots are situated on three circles of diameter 6, 7 and 8 mm centred on the optical zone. Using a ring electrode, the treatment could be carried out with different electrodes of different diameter. In order to study the effect of the electrode diameter on T_{max} and on the depth and width of the 40ºC isotherm line, we carried out computer simulations programming a 20 V output voltage during 1 s, and for three electrode diameters, 6, 7 and 8 mm. Table III shows the results. As the electrode diameter was increased from 6 to 8 mm, T_{max} decreased from 58.6 to 53.9ºC, the width of the 40ºC isothermal line decreased from 1112 to 925 μm, and the depth decreased from 480 to 392 μm. This result suggests that the change in electrode diameter has a significant effect on T_{max} and the temperature distributions. Moreover, there is a slight agreement between these results and those observed when the electrode thickness (S) was increased. In fact, both an increase of the electrode thickness (S) from 50 to 300 μm, and an increase of the electrode diameter (2·T) from 6 to 8 mm, produced similar changes in the 40ºC isothermal line dimensions (width decreased from 1070 to 911 μm when S increased, and from 1112 to 925 μm when 2·T increased; and depth decreased from 490 to 380 μm when S increased, and from 480 to 392 μm when 2·T increased). The cause of this agreement is that both changes (electrode thickness and electrode diameter) provoked an increase of the contact area, and thus a decrease of the current density.

However, when we studied the effect on T_{max}, a change in the electrode thickness was more significant than a change in the electrode radius: T_{max} decreased 19.2ºC for the change of S, and only 4.7ºC for the change of 2·T. Thus, the computer results of sections 3.3 and 3.4 indicated that the value of T_{max} is more sensitive to the change of electrode thickness than the change of electrode radius. Actually, if we consider the ring electrode a long electrode placed on the cornea and forming a loop, a change in its thickness (S in Fig. 2) means a change of the contact area between tissue and electrode but without variation of its entire length. On the contrary, a change in its diameter (2·T in Fig. 2) means a change of its entire length but without variation of its thickness.

We think that the higher current density located in the extremes of a long electrode owing to the edge effect is the underlying key in the behaviour of the ring electrodes. Moreover, and from this point of view, our results are in agreement with those obtained by LABONTÉ (1992). He proposed a theoretical model for RF cardiac ablation using a small dimensions electrode and studied the effect of the electrode contact area (electrode radius in his model and electrode thickness in our model). His results indicated a very marked increase of the tissue temperature when the contact area was decreased while output voltage was fixed.

In conclusion, our results suggest that when a ring electrode with bigger radius is used, lesion dimensions (width and depth) are reduced and T_{max} slightly decreases. In order to keep these dimensions balanced, it is possible to decrease the electrode thickness, although this fact involves a higher increase of T_{max}.

3.5 *Effect of electrode thermal conductivity*

In order to study the effect of the electrode thermal conductivity (k_e) on the temperature distributions, we made computer simulations (20 V, 1 s) using different values of k_e. We considered five cases: control case with an active electrode made of stainless steel (k_e=15 $W·m^{-2}·^oC^{-1}$), a platinum electrode (k_e=71 $W·m^{-2}·^oC^{-1}$), a gold electrode (k_e=317 $W·m^{-2}·^oC^{-1}$), and two cases with a very low thermal conductivity (1 $W·m^{-2}·^oC^{-1}$ and 0.1 $W·m^{-2}·^oC^{-1}$). Table IV shows the 40ºC isotherm line dimensions and T_{max} for several k_e considered. It can be observed that when k_e increased from 0.1 to 317 $W·m^{-2}·^oC^{-1}$, T_{max} decreased from 77.5 to 49.2ºC, the depth of the 40ºC isothermal line decreased from 517 to 375 μm, and its width decreased from 1118 to 800 μm. These results indicate that the change in k_e has a significant effect on the temperature distributions. The smallest dimension of the 40ºC isothermal line was obtained for the electrode with highest k_e. The T_{max} was also the lowest in this case.

Fig. 6 shows the temperature distributions at 1 s for different values of k_e. As can be seen in Fig. 6A, a very low value k_e (0.1 $W·m^{-2}·^oC^{-1}$) provoked a high thermal gradient located in the electrode body, and the RF energy placed in the cornea involved an important increase of T_{max}. On the contrary, when k_e increased to 1 $W·m^{-2}·^oC^{-1}$ (Fig. 6B) the thermal gradient in the electrode body decreased because it was easier to evacuate heat from the tissue, through the electrode, to the ambient. As a consequence, T_{max} also decreased.

In our study we observed a decrease of 40ºC isothermal line dimension when k_e was increased (Table IV). This result is not in complete agreement with that reported by SIMMONS *et al.* (1996) for RF cardiac ablation. They carried out an *in vitro* comparative study between two electrodes with different k_e. Using a constant power protocol, they found that the thermal lesions created using a 4 mm gold electrode were deeper than when using a 4 mm platinum electrode. The cause of the disagreement between their and our results is the programmed power level. When they used a low value of power, the platinum electrode created bigger lesions than the gold electrode. Under this condition, their and our results are in agreement. However, when power was increased, the lesions created with the platinum electrode were not fully completed, because a sudden rise of impedance occurred and the RF generator stopped the current delivery before the programmed time. They suggested that a high temperature in the tissue (T>100ºC) could provoke this fact. For this reason, the lesions did not grow enough, and were smaller than the lesions created with the gold electrode.

Besides, Fig. 6 also shows the location of T_{max} for each case. When k_e increased from 0.1 to 317 $W \cdot m^{-2} \cdot {}^{o}C^{-1}$, its location moved away to the outer zone ≈150 μm and slightly to the deeper zone. A similar effect was observed in experimental and theoretical studies using irrigated tip electrodes and constant voltage to create larger lesions. NAKAGAWA *et al.* (1995) observed that the RF current delivery using non-irrigated electrodes terminated prematurely due to an impedance rise. This fact was provoked by temperatures of nearly 100ºC at the tip of the electrode. On the contrary, the use of irrigated electrodes allowed producing larger lesions because the location of the maximal temperature (≈100ºC) shifted from the electrode tip to a deeper zone of the tissue. CURLEY and HAMILTON (1997) studied the temperature distribution during RF heating using a theoretical model and they obtained a similar result. Their computer simulations indicated that when an irrigated electrode is used, the location of the maximal temperature shifted towards a deeper zone compared to a non-irrigated electrode. It is known that this is due to the better capability of the electrode body to remove the heat away from the tissue. Although our electrode is not irrigated, the displacement of T_{max} observed in a ring electrode when k_e is increased, is similar to obtained in an irrigated electrode when the flow rate is increased.

Finally, during RF-TKP, it is necessary to create deep lesions in the cornea. The CK procedure clinically used and reported by ASBELL *et al*. (2001) is based on a self-limiting process in order to create lesions with a depth less than 80% of corneal thickness: the CK procedure delivers RF current and the collagen dehydrates; this provokes an increase of the resistance to the current flow and the RF generator stops. However it is known that, on one hand, the tissue dehydration is related to high values of temperature (≈100ºC), and on the other hand, an excessive value of T_{max} in the cornea collagen could cause a regression in the therapeutic result of the refractive correction (MCCALLY *et al.*, 1983). As a consequence, we think that the use of a ring electrode with a high k_e could create lesions with enough depth, avoiding the self-limiting process and a value of T_{max} ≈100ºC in the cornea collagen.

3.6 *In vitro experiments*

Five lesions were created in rabbit eyes. Only one lesion was made in the centre of the eye using a RF power of 5 W and a programmed duration of 20 s. Table V shows the resulted macroscopic and microscopic characteristics of the thermal lesions. The most important conclusion is that the proposed ring electrode can create fully circular thermal lesions. Attachment of the ring electrode to the tissue after RF heating occurred in 4 of 5 cases. Three of 4 corneas heated during 20 s (eyes #1, #2 and #4) showed a lesion depth of 60% of cornea thickness (see Fig. 7-bottom), while the cornea of eye #5 showed a lesion depth between 60 and 80%. On the contrary, the cornea heated during 10 s (eye #3), achieved only a depth between 30 and 40% in accordance with the zone analysed (see Fig. 7-top). The cause of this smaller lesion depth could be the well known fact that the heating duration has a direct and significant effect on the lesion dimension during the first seconds (LABONTÉ, 1994; JAIN and WOLF, 1999).

The difference of lesion depth in different zones of the eye #3 indicates that it was not uniform across the circular path. The same fact was observed in the eye #5 as can be seen in Fig. 8. The lesion depth was different in accordance with the cornea fragments analysed: 60% in fragment A and 80% in fragment B. We think that this fact may be due to a non uniformity of several parameters across the circular pattern. We suggest two parameters: a) the contact pressure between electrode and tissue, and b) the biological dispersion in the values of the electrical, thermal and mechanical characteristics of the cornea. In fact, theoretical (JAIN and WOLF, 1998; BERJANO *et al.*, 2002) and experimental (AVITALL *et al.*, 1997) studies have demonstrated that the electrode-tissue pressure has a significant effect on the temperature profile and thereby on the lesion dimension. Equally, other studies have showed the significant effect of the biological dispersion of the electrical and thermal characteristics of the tissue (TUNGJITKUSOLMUN *et al.*, 2000; BERJANO *et al.*, 2002), and of the tear film (MENDEZ-G and MENDEZ-NOBLE, 1997; BERJANO *et al.*, 2002).

The experimental results showed fully circular thermal lesions with semi-torus shape, and in this respect, there was an agreement between the lesion morphology obtained theoretically and experimentally. Moreover, the histological analysis showed that in all the *in vitro* lesions the coagulation contour located near the central stromal. Since BRICKMANN *et al.* (1996) have shown that this coagulation contour observed on the histological samples occurs in a temperature range around 100ºC using short heating times, our experimental results suggest that in all the lesions the critical shrinkage temperature (55-63ºC) was reached at central stromal thickness.

3.7 *Limitations of the theoretical model*

Although we have observed an agreement between the lesion shape obtained theoretically and experimentally, the used numerical model has two main limitations. On one hand, we have not modelled the strong change in the mechanic characteristics of the cornea during the heating (STRINGER and PARR, 1964). On the other hand, there are no experimental data about the change in the thermal and electrical characteristics of the cornea under strong desiccation conditions. For this reason, future studies should investigate more realistic models including the behaviour of the interface tissue-electrode under high temperature conditions and strong tissue desiccation, such as CHOI *et al*. (2002) have suggested. In spite of the limitations, the proposed numerical model qualitatively predicts the process of heating of the cornea using a RF ring electrode, and thereby it could be used in order to study the effect of different electrode designs or application modes (voltage, current or power constant) on the temperature distributions.

3.8 *Limitations of the study and clinical implications*

Experimental studies have demonstrated that the application of heated brass rings on the cornea induced a significant increase of corneal curvature (MILLER and MANNING, 1978; GRUENBERG *et al.,* 1981). However, the changes of corneal refracting power obtained by GRUENBERG *et al.* (1981) in living rabbits tended to be transient. This was probably due to the central stroma not reaching the critical shrinkage temperature. When heated probes are applied on the cornea, the thermal energy is conducted from the surface towards the corneal stroma. On the contrary, RF energy is directly dissipated inside the tissue; and the electrode acts as a heat sink, effectively pushing the hot spot deeper inside the tissue. These two effects combine to produce a higher temperature elevation at depth and conceivably a deeper lesion (LABONTÉ, 1992). In this respect, our theoretical results indicate that the lesions created by the ring electrode had a fully circular shape. In addition, our experimental results showed *in vitro* lesions sufficiently deep along the entire circular path. As a consequence, we think that the use of a RF ring electrode could minimise the drawbacks found by GRUENBERG *et al.* (1981). Nevertheless, this issue should be assessed in future investigations.

The previous work on heated brass rings suggests that the creation of a sufficiently deep fully circular lesion would overcome the current limit of +3.00 diopters in hyperopia correction. Moreover, it is known that in CK procedure there is a direct relationship between the number of lesion spots created at each optical zone and the number of diopters to correct (MÉNDEZ-G and MÉNDEZ-NOBLE, 1977; ASBELL *et al.*, 2001). For this reason, if a fully circular lesion is considered like an extreme case of an optical zone with many lesion spots, it would be possible to think that the use of the RF ring electrode could increase the maximum number of diopters corrected by CK using a single probe. Other techniques such as the laser in situ keratomileusis (LASIK) allow to correct hyperopia up to +6.00 diopters (MANNIS *et al.*, 2001). However, the heating systems using low frequency RF (300 kHz – 1 MHz) currents are a low cost option as opposed to other heating systems for TKP based on laser (SEILER *et al.*, 1990), microwave (TREMBLY and KEATES, 1991) or ultrasound (RUTZEN *et al.*, 1990).

Previous studies performed by the authors (ALIÓ *et al.*, 1999) with laser thermal keratoplasty (LTK) on human eyes for the correction of hyperopia, a technique that has the same purpose as CK, have proved that the outcome is very frequently affected by regression and induced astigmatism. The main cause of this astigmatism is the lack of symmetry in the energy delivered in different spots placed at the cornea in different moments during the surgery (ALIÓ *et al*., 1997a; ALIÓ *et al*., 1997b; ALIÓ *et al*., 1999; ALIÓ *et al*., 2002). In our study, the histopathologic pattern observed in the *in vitro* lesions was similar along the circular trajectory, on the contrary of what is found in LTK (AYALA *et al*., 2000).

In our study, in 2 eyes the lesions had different depth along the circular pattern. We have suggested that this is could be due to a non uniformity of several parameters across the circular pattern (see section 3.6). For this reason, future studies on the ring electrode should include technical improvements in order to minimise the effect of these parameters as far as possible. For instance, it could be useful to match the pressure between electrode and cornea in all the contact area, and to homogenize the hydration on the cornea surface before the heating. As a consequence, if the ring electrode would be technically improved, it could deliver RF energy at the same moment along the whole area of contact with the cornea, and therefore it could minimise or even cancel the induction of astigmatism. Moreover, circular probes adequately configured in oval shapes could also be useful in the correction of astigmatism, a fact that is not possible to be approached at this moment with the current methods of LKT or CK available.

In order to investigate the potential and limitation of a new electrode for RF heating of the cornea, we have used mathematical modelling and *in vitro* experiments. Although theoretical models for RF heating are a powerful tool for predicting lesion dimension created by different electrode designs under different tissue characteristics or environment conditions, our study is only a first step in the research and development of a new device. Consequently, future research should, on one hand, quantify the change in corneal curvature in all the meridians induced by the ring electrode; and on the other hand, assess the potential risks originated from the creation of a fully circular thermal lesion. The final goal should be the validation of the electrode for its clinical use, and particularly, for its possible application with oval shape in correction of several types of astigmatism.

4 Conclusions

We have presented a numerical model for the study of RF-TKP using a ring electrode of surface application. We studied the electro-thermal behaviour of the ring electrode and we observed a non symmetric distribution of electrical field in the tissue. The results showed a higher value in the cornea zone located near the outer perimeter of the electrode. This effect provoked a higher temperature in that zone. However, the lesions had a semi-torus shape. Moreover, our results also showed that the electrode thermal conductivity, the electrode radius and the electrode thickness had a significant effect on the maximal temperature achieved in the tissue.

We carried out *in vitro* experiments using a model based on a rabbit eye. The experimental results indicated that at a 5 W power, the ring electrode was able to create fully circular thermal lesions with semi-torus shape, thus, there was an agreement between the lesion morphology obtained theoretically and experimentally. We also observed that some lesions showed non uniform characteristics along their circular path. Lesion depth depended on heating duration (60% of corneal thickness for 20 s, and 30% for 10 s). The experimental results suggest that the critical shrinkage temperature (55-

63ºC) was reached at the central stroma in all the cases and along the entire circular path.

Acknowledgment -- The authors wish to thank Mr. Pedro Más for his technical assistance in building the ring electrodes, Mr. Wouter Vlaanderen and Ms. Chris Guevara for the suggestions they provided, and the reviewers for their helpful comments.

This work was partially supported Instituto de la Mediana y Pequeña Empresa de Valencia (IMPIVA)–Generalitat Valenciana under Ref: 971701003827, Universidad Politécnica de Valencia (Programa de Incentivo a la Investigación), and Mercé V. Electromedicina S.L. (Valencia, Spain).

References

ALIÓ, J. L., ISMAIL, M. M., ARTOLA, A., and PÉREZ-SANTONJA, J. J. (1997a): "Correction of hyperopia induced by photorefractive keratectomy using non-contact Ho: YAG laser thermal keratoplasty", *J. Refract. Surg.*, **13**, pp. 13-16.

ALIÓ, J.L., ISMAIL, M. M., and SANCHEZ, J. L. (1997b): "Correction of hyperopia with non-contact Ho: YAG laser thermal keratoplasty", *J. Refract. Surg.*, **13**, pp. 17-22.

ALIÓ, J. L., and PÉREZ-SANTONJA, J. J. (1999): "Correction of hyperopia by laser thermokeratoplasty (LTK)" in PALLIKARIS, I., and AGARWAL, S. (Eds.): "Refractive Surgery" (Jaypee Brothers Medical Publishers Ltd., New Delhi), pp. 583-591.

ALIÓ, J. L., and PÉREZ-SANTONJA, J. J. (2002): "Corrrection of hyperopia by laser thermokeratoplasty (LTK)" in AGARWAL, S., AGARWAL, A., APPLE, D. J., BURATTO, L., ALIÓ, J. L., PANDEY, S. K., and AGARWAL, A. (Eds.): "Textbook of Ophthalmology" (Lippincott Williams & Wilkins, Philadelphia), pp. 1331-1337.

AYALA, M. J., ALIÓ, J. L., ISMAIL, M. M., and SÁNCHEZ-CASTRO, J. M. (2000): "Experimental corneal histological study after thermokeratoplasty with holmium laser", *Arch. Soc. Esp. Oftalmol.*, **75**, pp. 619-626.

ASBELL, P. A., MALONEY, R. K., DAVIDORF, J., HERSH, P., MCDONALD, M., MANCHE, E., and CONDUCTIVE KERATOPLASTY STUDY GROUP (2001): "Conductive keratoplasty for the correction of hyperopia", *Tr. Am. Ophtalmol. Soc.*, **99**, pp. 79-87.

AVITALL, B., MUGHAL, K., HARE, J., HELMS, R., and KRUM, D. (1997): "The effects of electrode-tissue contact on radiofrequency lesion generation", *PACE*, **20**, pp. 2899-2910.

AVITALL, B., HELMS, R. W., KOBLISH, J. B., SIEBEN, W., KOTOV, A. V., and GUPTA, G. N. (1999): "The creation of linear contiguous lesions in the atria with an expandable loop catheter", *J. Am. Coll. Cardiol.*, **33**, pp. 972-984.

BERJANO, E. J., SAIZ, J., and FERRERO, J.M. (2002): "Radio-frequency heating of the cornea: Theoretical model and *in vitro* experiments", *IEEE Trans. Biomed. Eng.*, **49**, pp. 196-205.

BRICKMANN, R., KAMPMEIER, J., GROTEHUSMANN, U., VOGEL, A., KOOP, N., ASIYO-VOGEL, M., KAMM, K., and BIRNGRUBER, R. (1996): "Corneal collagen denaturation in laserthermokeratoplasty", *SPIE Proc.*, **2681**, pp. 56-63.

CHOI, B., KIM, J., WELCH, A. J., and PEARCE, J. A. (2002): "Dynamic impedance measurements during radio-frequency heating of cornea", *IEEE Trans. Biomed. Eng.*, **49**, pp. 1610-1616.

CURLEY, M. G., and HAMILTON, P. S. (1997): "Creation of large thermal lesions in liver using saline-enhanced RF ablation" Proc. 19th Ann. Int. Conf. IEEE Eng. Med. Biol. Soc. Chicago (IEEE Piscataway NJ) pp. 2516-2519.

DOSS, J. D., and ALBILLAR, J. I. (1980): "A technique for the selective heating of corneal stroma", *Contact Intraocular Lens Med.*, **6**, pp. 13-17.

DOSS, J. D. (1982): "Calculation of electric fields in conductive media", *Med. Phys.*, **9**(4), pp. 566-573.

GRUENBERG, P., MANNING, W., MILLER, D., and OLSON, W. (1981): "Increase in rabbit corneal curvature by heated ring application", *Ann. Ophthalmol.*, **13**, pp. 67-70.

HATA, C., and RAYMOND CHIA, W-K. (2001): "Catheter for circular tissue ablation and methods thereof". US Patent 2001/0044625 A1.

JAIN, M. K., and WOLF, P. D. (1998): "Effect of electrode contact on lesion growth during temperature controlled radiofrequency ablation", Proc. 20th Ann. Int. Conf. IEEE Eng. Med. Biol. Soc. Hong Kong (IEEE Piscataway NJ) pp. 245-247.

JAIN, M. K., and WOLF, P. D. (1999): “Temperature controlled and constant power radiofrequency ablation: what´s affects lesion growth?”, *IEEE Trans. Biomed. Eng.*, **46**, pp. 1405-1412.

KRASTEVA, V. TZ., and PAPAZOV, S. P. (2002): “Estimation of current density distribution under electrodes for external defibrillation”, *Biomed. Eng. OnLine*, **1**:7.

LABONTÉ, S. (1992): “A Theoretical study of radio-frequency ablation of the myocardium”, *Ph.D. dissertation*, Dep. Elec. Eng, Univ. Ottawa, Canada.

LABONTÉ, S. (1994): “Numerical model for radio-frequency ablation of the endocardium and its experimental validation”, *IEEE Trans. Biomed. Eng.*, **41**, pp. 108-115.

MANNIS, M. J., SEGAL, W. A., and DARLINGTON, J. K. (2001): “Making sense of refractive surgery in 2001: Why, when, for whom, and by whom?”, *Mayo Clin. Proc.*, **76**, pp. 823-829.

MCCALLY, R. L., BARGERON, R. A., and GREEN, W. R. (1983): “Stromal damage in rabbit corneas exposed to CO2 laser radiation”, *Exp. Eye Res.*, **37**, pp. 543-550.

MCDONALD, M. B., HERSH, P. S., MANCHE, E. E., MALONEY, R. K., DAVIDORF, J., and SABRY, M. (2002): “Conductive keratoplasty for the correction of low to moderate hyperopia: U.S. clinical trial 1-year results on 355 eyes”, *Ophthalmol.*, **109**, pp. 1978-1989.

MCRURY, I. D., MITCHELL, M. A., PANESCU, D., and HAINES, D. E. (1997): “Non-uniform heating during radiofrequency ablation with long electrodes: monitoring the edge effect”, *Circ.*, **96**, pp. 4057-4064.

MÉNDEZ-G, A., and MÉNDEZ-NOBLE, A. (1997): “Conductive keratoplasty of the correction of hyperopia” in SHER, N.A. (Ed.): “Surgery for Hyperopia and

Presbyopia" (Williams & Wilkins, Baltimore), pp. 163-171.

MILLER, D., and MANNING, W.J. (1978): "Alterations in curvature of bovine cornea using heated rings", *Invest. Ophthalmol.*, (suppl), April, p. 297.

MIROTZNIK, M. S., and SCHWARTZMAN, D. (1996): "Nonuniform heating patterns of commercial electrodes for radiofrequency catheter ablation", *J. Cardiovasc. Electrophysiol.,* **7**, pp. 1058-1062.

NAKAGAWA, H., YAMANASHI, W. S., PITHA, J. V., ARRUDA, M., WANG, X., OHTOMO, K., BECKMAN, K. J., MCCLELLAND, J. H., LAZZARA, R., and JACKMAN, W. M. (1995): "Comparison of in vivo tissue temperature profile and lesion geometry for radiofrequency ablation with a saline-irrigated electrode versus temperature control in a canine thigh muscle preparation" *Circ.*, **91**, pp. 2264-2273.

PANESCU, D., WHAYNE, J. G., FLEISCHMAN, S. D., MIROTZNIK, M. S., SWANSON, D. K., and WEBSTER, J. G. (1995): "Three-dimensional finite element analysis of current density and temperature distributions during radio-frequency ablation", *IEEE Trans Biomed Eng.*, **42**, pp. 879-890.

PLONSEY, R., and HEPPNER, D. B. (1967): "Considerations of quasi-stationarity in electrophysiological systems", *Bull Mathematical Biophysics*, **29**, pp. 657-664.

ROWSEY, J. J. (1987): "Electrosurgical keratoplasty: Update and retraction", *Invest. Ophthalmol. Vis. Sci.*, **28**, p. 224.

RUTZEN, A. R, ROBERTS, C. W., DRILLER, J., GOMEZ, D., LUCAS, B. C., LIZZI, F. L., and COLEMAN, D. J. (1990): "Production of corneal lesions using high-intensity focused ultrasound", *Cornea*, **9**, pp. 324-330.

SCHWAN, H. P., and FOSTER, K. R. (1980): "RF-fields interactions with biological systems: electrical properties and biophysical mechanism", *Proc. IEEE*, **68**, pp. 104-

113.

SEILER, T., MATALLANA, M., and BENDE, T. (1990): “Laser thermokeratoplasty by means of a pulsed Holmium:YAG Laser for the hyperopic correction”, *Refrac. Corneal Surg.*, **6**, pp. 335-339.

SILVESTRINI, T. A. (1998): “Electrosurgical procedure for the treatment of the cornea”, US Patent 5,766,171.

SIMMONS, W. N., MACKEY, S., HE, D. S., and MARCUS, F. I. (1996): “Comparison of gold versus platinum electrodes on myocardial lesion size using radiofrequency energy”, *PACE*, **19**, pp. 398-402.

STRINGER, H., and PARR, J. (1964): “Shrinkage temperature of eye collagen”, *Nature*, **204**, p. 1307.

TREMBLY, B. S., and KEATES, R. H. (1991): “Combined microwave heating and surface cooling of the cornea”, *IEEE Trans. Biomed. Eng.*, **38**, pp. 85-91.

TREMBLY, B. S., HASHIZUME, N., MOODIE, K. L., COHEN, K. L., TRIPOLI, N. K., and HOOPES, P. J. (2001): “Microwave thermal keratoplasty for myopia: keratoscopic evaluation in porcine eyes”, *J. Refract. Surg.*, **17**, pp. 682-688.

TUNGJITKUSOLMUN, S., WOO, E. J., CAO, H., TSAI, J. Z., VORPERIAN, V. R., and WEBSTER, J. G. (2000): “Thermal-electrical finite element modelling for radio frequency cardiac ablation: effects of changes in myocardial properties”, *Med. Biol. Eng. Comput.*, **38**, pp. 562-568.

WILEY, J. D., and WEBSTER, J. G. (1982): “Analysis and control of the current distribution under circular dispersive electrodes”, *IEEE Trans. Biomed. Eng.*, **29**, pp. 381-385.

Appendix

The temperature distribution in the model was obtained by solving the bio-heat equation (JAIN and WOLF, 1999)

$$\rho \cdot c \cdot \frac{\partial T}{\partial t} = \nabla \cdot k \nabla T + q - Q_p + Q_m \tag{2}$$

where ρ is the mass density (kg·m^{-3}), c is the specific heat capacity (J·kg^{-1}·K^{-1}), k is the thermal conductivity (W·m^{-1}·K^{-1}), T is the temperature (ºC), q is the heat source (W·m^{-3}), Q_p is the perfusion heat loss (W·m^{-3}), and Q_m is the metabolic heat generation (W·m^{-3}). The situation was simplified by ignoring Q_p and Q_m as they are negligible for RF heating (JAIN and WOLF, 1999).

At the frequencies (500 kHz) and over the distance of interest (the electrical power is deposited in a small radius around the active electrode) the medium can be considered resistive, because the displacement currents can be neglected. Therefore, it is possible to use a quasi-static approach to the electrical problem (PLONSEY and HEPPNER, 1967; DOSS, 1982). The distributed heat source (Joule loss) is given by

$$q = \boldsymbol{J} \cdot \boldsymbol{E} \tag{3}$$

where $\boldsymbol{J}$ is the current density (A·m^{-2}), and $\boldsymbol{E}$ is the electric field intensity (V·m^{-1}). These were evaluated using Laplace's equation

$$\nabla \cdot \sigma \nabla V = 0 \tag{4}$$

where V is the root mean squared (r.m.s.) voltage (V) and σ is the electrical conductivity (S·m^{-1}).

TABLE I

CHARACTERISTICS OF THE MATERIALS USED IN OUR THEORETICAL MODEL

σ: ELECTRICAL CONDUCTIVITY; ρ: MAS DENSITY; c: SPECIFIC HEAT; AND k: THERMAL CONDUCTIVITY

MATERIAL	σ ($S \cdot m^{-1}$)	ρ ($kg \cdot m^{-3}$)	c ($J \cdot kg^{-1} \cdot K^{-1}$)	k ($W \cdot m^{-1} \cdot K^{-1}$)
Cornea	2.56 [(1)]	1000	3830	0.556
Aqueous humor	1.6 [(1)]	1000	4180	0.578
Electrode	7.4E+6	8E+3	480	15

[(1)] Frequencies of measurement: 10 kHz -10 MHz.

TABLE II

EFFECT OF THE RING ELECTRODE THICKNESS ON MAXIMUM TEMPERATURE REACHED IN THE TISSUE (T_{max}) AND ON THE DEPTH AND WIDTH OF THE 40ºC ISOTHERM LINE. SIMULATIONS USING 20 V AND 1 s

Electrode thickness (μm)	**T_{max} (ºC)**	**Width (μm)**	**Depth (μm)**
50	71.6	1070	490
100	63.6	1000	436
200	55.2	933	400
300	50.4	911	380

TABLE III

EFFECT OF THE RING ELECTRODE DIAMETER ON MAXIMUM TEMPERATURE REACHED IN THE TISSUE (T_{max}) AND ON THE DEPTH AND WIDTH OF THE 40ºC ISOTHERM LINE. SIMULATIONS USING 20 V AND 1 s

Electrode diameter (mm)	**T_{max} (ºC)**	**Width (μm)**	**Depth (μm)**
6	58.6	1112	480
7	55.2	933	400
8	53.9	925	392

TABLE IV

EFFECT OF THE RING ELECTRODE THERMAL CONDUCTIVITY (k) ON MAXIMUM TEMPERATURE REACHED IN THE TISSUE (T_{max}) AND ON THE DEPTH AND WIDTH OF THE 40ºC ISOTHERM LINE. SIMULATIONS USING 20 V AND 1 s

k (W·m^{-1}·ºC^{-1})	**T_{max} (ºC)**	**Width (μm)**	**Depth (μm)**
0.1	77.5	1118	517
1	69.0	1117	482
15 (Control case. Stainless steel)	55.2	933	400
71 (Platinum)	50.6	872	390
317 (Gold)	49.2	800	375

TABLE V

MACROSCOPIC AND MICROSCOPIC CHARACTERISTICS OF THE THERMAL LESIONS CREATED USING A RING ELECTRODE AND 5 W POWER

Eye	time (s)	MICROSCOPIC ASSESSMENT Lesion depth **	MACROSCOPIC ASSESSMENT
#1	20	60 %	F-C-V ; A-E-C
#2	20	60 %	F-C-V ; A-E-C
#3	10 *	30 - 40 %	F-C-V ; A-E-C
#4	20	60 %	F-C-V ; NON A-E-C
#5	20	60 – 80 %	F-C-V ; A-E-C

F-C-V: Fully circular and visible lesion. **A-E-C**: Attachment of the electrode to the cornea after the RF heating. (*) The RF delivery stopped because the impedance increased suddenly.

(**) Lesion depth given as a percentage of corneal thickness.

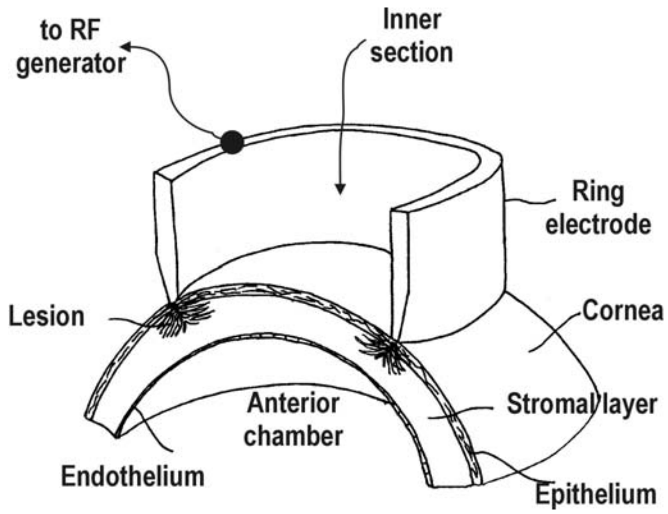

Figure 1. Physical situation considered in the study of the radiofrequency thermokeratoplasty using a ring electrode. Names of model elements are printed in bold.

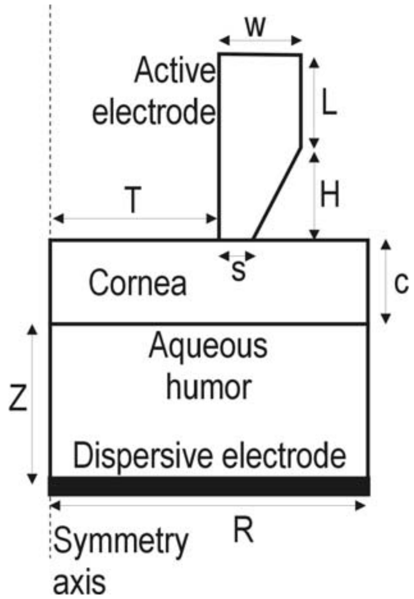

Figure 2. Theoretical model proposed (out of scale). Nomenclature: Z and R: outer dimensions of the model; S: active electrode thickness in contact zone; T: electrode radius; W: thickness of the electrode body; H: length of the sharp-edge zone of the active electrode; L: length of the active electrode included in the model; and C: corneal thickness.

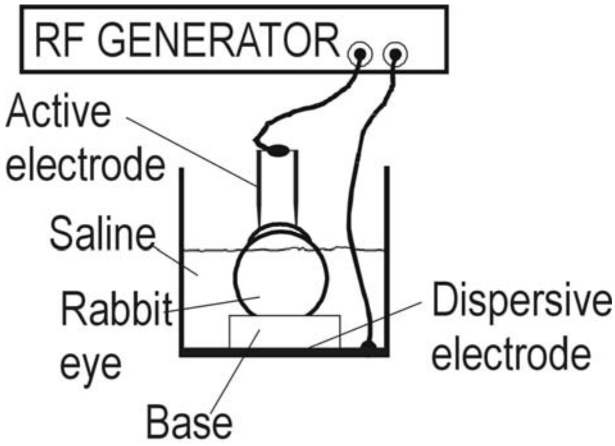

Figure 3. *In vitro* model used in the experiments.

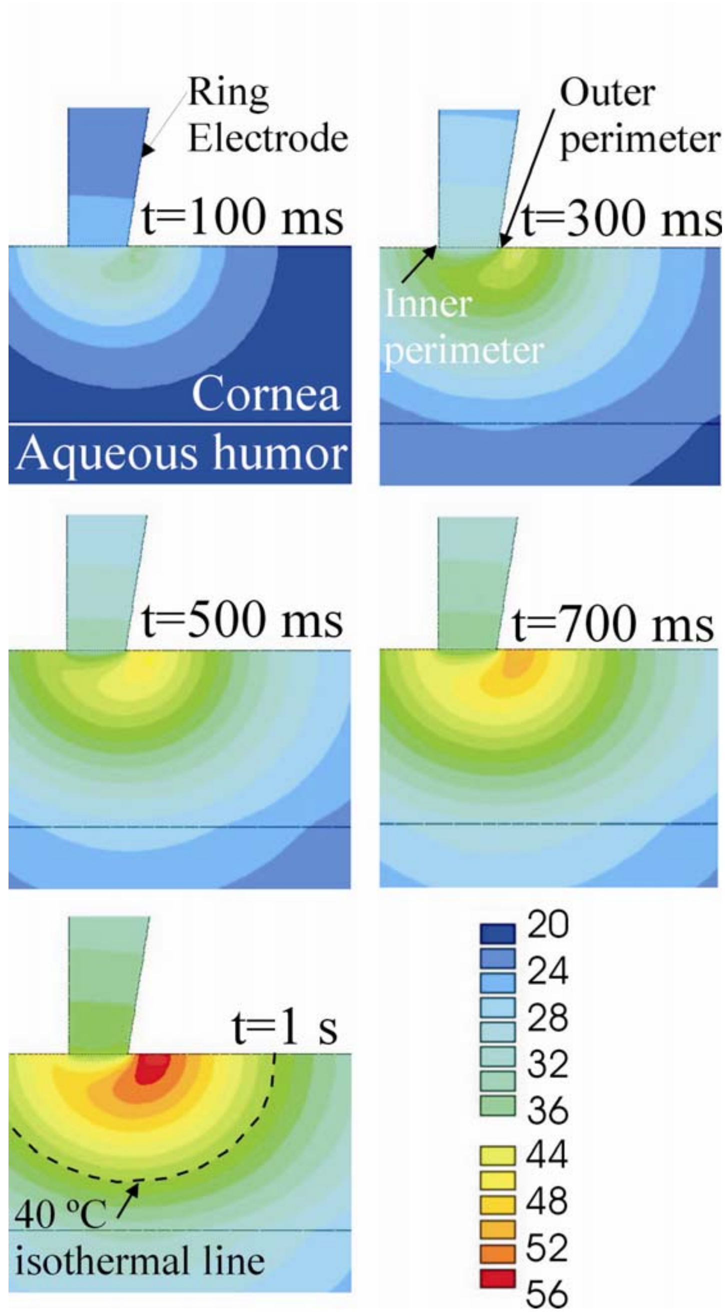

Figure 4. Temperature distribution maps near the interface electrode-cornea computed from the theoretical model showed in Fig. 2 for several times. Programmed voltage of 20 V during 1 s. Temperature scale is in ºC.

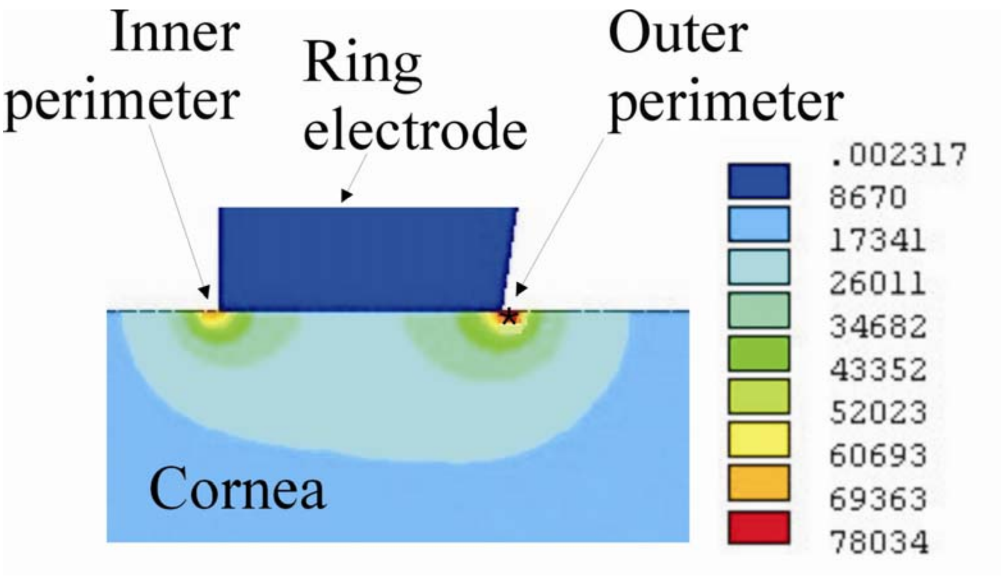

Figure 5. Spatial distribution of electric field near the interface electrode-cornea at t = 1 s (programmed voltage of 20 V). Computed from the theoretical model showed in Fig. 2. Scale is in V/m. Symbol "*" indicates the location of maximal value.

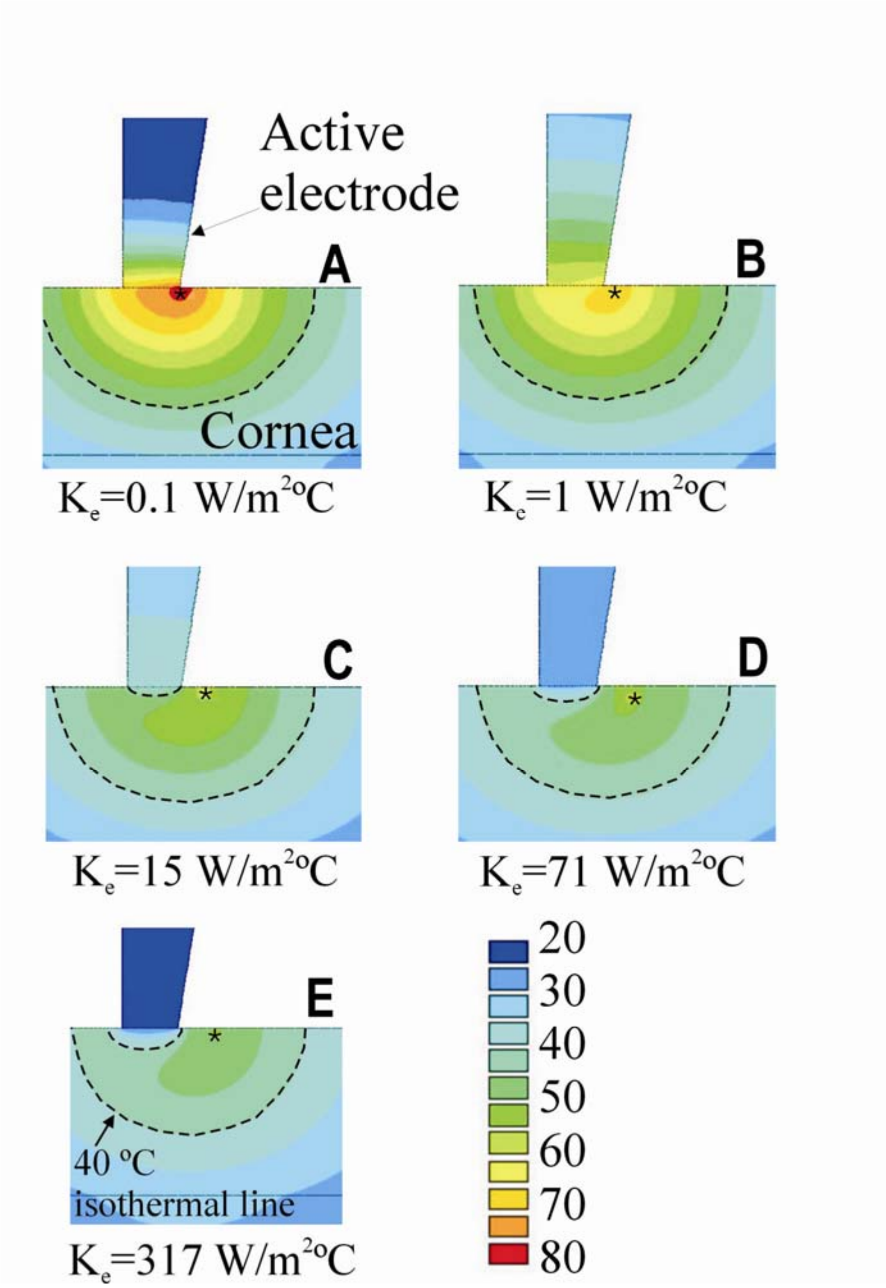

Figure 6. Temperature distributions in the cornea for different values of thermal conductivity of the ring electrode. Programmed voltage of 20 V during 1 s. Temperature scale is in ºC. Symbol "*" indicates the location of maximal temperature.

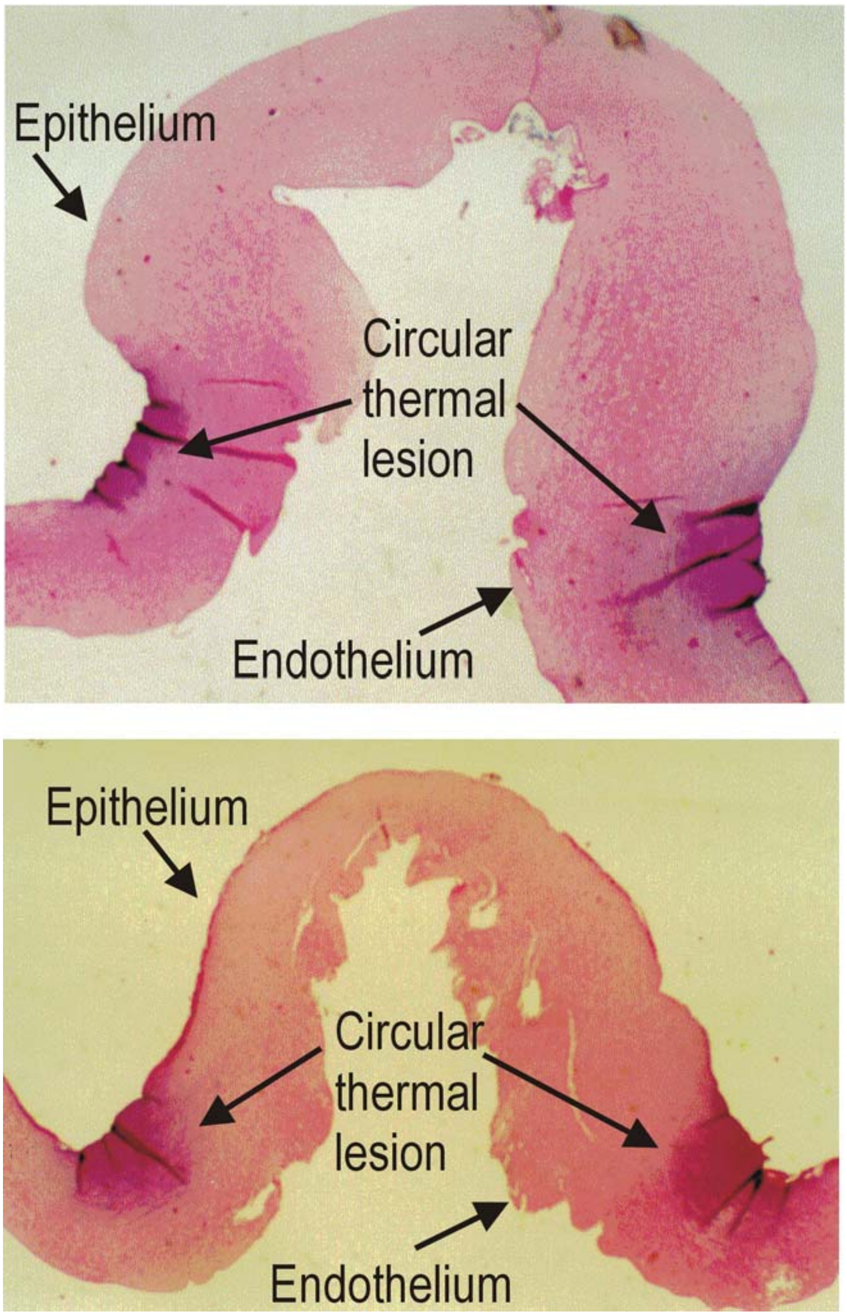

Figure 7. Cross-sections of rabbit corneas heated with a ring electrode of 200 μm thickness and 7 mm diameter (hematoxylin and eosin, ×100). Top: lesion created with 5 W power during 10 s (eye #3). Bottom: lesion created with 5 W power during 20 s (eye #2).

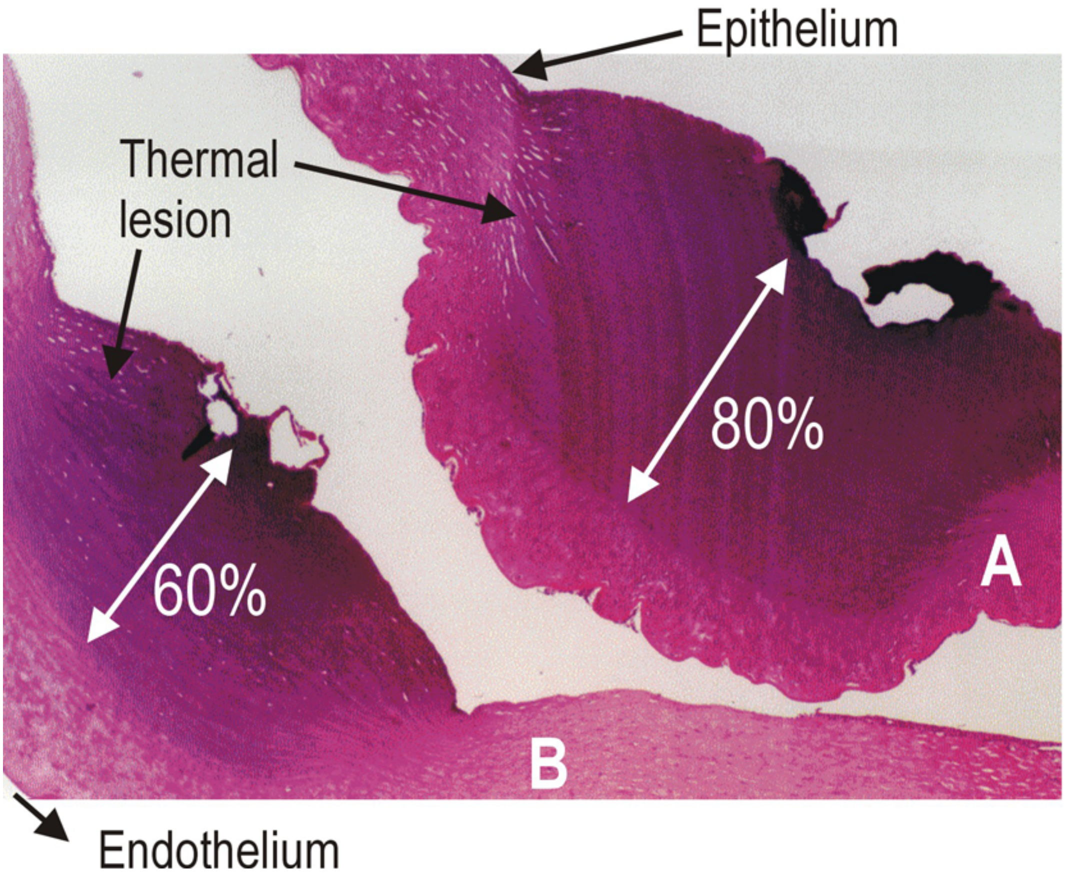

Figure 8. Two opposite cross-sections (A and B) of a same rabbit cornea heated with a ring electrode of 200 μm thickness and 7 mm diameter (hematoxylin and eosin, ×100). Lesion created with 5 W power during 20 s (eye #5).